OnLine Journal of Earth Sciences 11 (1): 1-9, 2017
ISSN: 1991-7708

Mineral Chemistry and Temperature Determination of Skarn Formation in Dezg Area, Southwestern of Hajiabad, North of Birjand

[1]Zohreh Esmaeili, [2]Gholamreza Fotohirad and [2]Mohammad Hossein Yousefzadeh
[1]Department of Geology, University of Birjand, Birjand, Iran
[2]Department of Mining Engineering, University of Birjand, Birjand, Iran

Abstract: The study area is located in North of Dezq village in southwestern of Hagiabad. Mineralogical and geochemical investigations is showing two main stage of prograde and retrograde metamorphism in formation of skarn in study area. In prograde stage has formed skarn with anhydrous silicate-calcium mineral assemblage (andradite-grossular and diopside-hedenbergite) in temperature range of 328-599° which has similar composition with garnets from Cu-Fe and Au skarns. In retrograde stage, a part of these anhydrous silicates are affected by retrograde metamorphism and changed to hydrous and anhydrous silicate minerals with less calcium (epidote, tremolite-actinolite) and finally hydrous and anhydrous calcium assemblage has altered to fine grain minerals including chlorite, calcite, quartz and clay minerals in temperature range of >300°.

Key words: Skarn, garnet, prograde metamorphism, retrograde metamorphism, Sistan suture

INTRODUCTION

The study area (near the village of Dezg) is a part of Sistan suture zone in the East (Eastern Mountains) of Iran extending from North West to southeast and located near the village of Surand. Dezg is located in the southwest of Hajiabad at within the longitudes of 60°0657.47-60°0411.11 east and latitudes of 33°2025.27-33°2202.93 North on Shahrokht map 1:250000 and Ahangaran map 1:100000. In most tectonic-sedimentary classifications, this part of Iran has been introduced as Sistan structural zone. Sistan suture zone is another name that researchers have used for this area (Tirrul *et al*., 1983). Located in the east vicinity of the study area, the region's highlands are made of lime stones as old as lower cretaceous and paleocene (Rad *et al*., 2004, 2005; Angiboust *et al*., 2013; Brocker *et al*., 2013). In the South of the region, an assemblage of tonalite igneous rocks and granodiorite can be seen and the West is covered with igneous rocks belonging to ophiolite complex that are mostly peridotite. Among the metamorphic rocks observed in the region are granilita, amphibolite, epidote amphibolite, green schist and skarn (Esma'ili, 2014). The present investigation's main aim was the study of mineral chemistry and temperature of skarn formation.

Geology of the region: The study region is a part of Sistan suture zone in the East of Iran that extends from North West to Southeast on Shahrokht map 1:250000 (Fig. 1). In fact, the study region is an ophiolite complex that is an almost complete sequence of ultramafic to mafic igneous rocks (partially metamorphic) and radiolarian cherts and radiolarites (partly metamorphic) and has a certain metamorphic zone in the Eastern part. The above rock complex is interdigitally located in relation to one another and to other components of the ophiolite complex.

Ophiolite sequence is not well observable due to bearing of different tectonic activities. In some points of the region; however, almost no specific sequence can be seen. In these points, metamorphic zone rocks to ultramafic rocks, gabbro, very specific metamorphosed sheet dikes, basalt to andesite basalt and a specific bedding can be observed in gabbroic rocks.

In the south of the region, there is an assemblage of tonalite and granodiorite igneous rocks and formation of skarn can be as a result of adjacency of this intrusive body with rocks containing skarn in further depth and the formed skarn comes to the surface of the ground. Mineralogical examination is an important tool in identifying and determining the type of the skarns. Moreover, mineralogy is an important factor to figure out the origin of the skarns and the formation temperature and identification of minerals with economic value. Due to its combination with other suitable minerals, garnet acts as a good geothermobarometry. In general, calcic skarns form from metasomatism of limestones in final stages of replacement of an intrusion at shallow depths. Main minerals of calcic skarns include garnet (Grossular Andradite), clinopyroxene (diopside-hedenbergite), epidote, vesuvianite, scapolite, wollastonite, magnetite,

Corresponding Author: Zohreh Esmaeili, Department of Geology, University of Birjand, Birjand, Iran

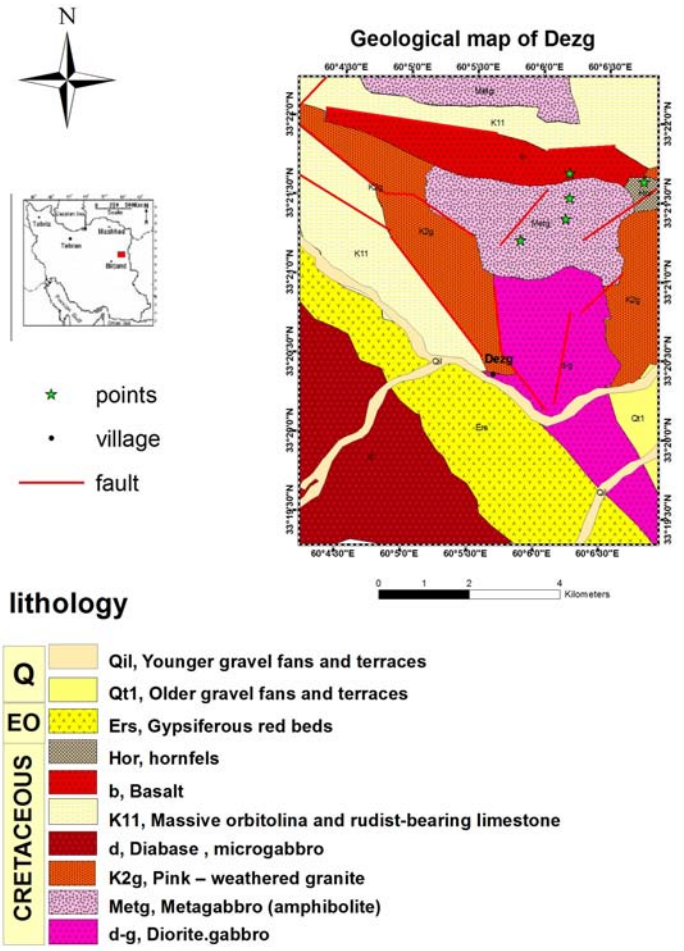

Fig. 1: The geological map of the study region

etc. which are identifiable depending on the transformation degree and the effects of processes of retrograde metamorphism on the aureole formed at the metamorphic peak in different zones. Petrographic studies and also fluid inclusion studies play an important role in understanding skarn formation process and the path taken in pressure-temperature diagram.

MATERIALS AND METHODS

In the present study, a reference (Esma'ili, 2014) was used to collect the required data. After relevant reports, maps and studies were examined, field observations were made several times in order to examine border of rock units, collect samples and take photos.

Afterwards, among the 176 collected sample rocks (Esma'ili, 2014); 116 samples with thin section and 16 samples with polished section were prepared and examined with polarizing microscope and reflected light (Table 1). In these examination, different mineral collections were identified in metamorphic rocks in order to determine the metamorphic face and examination of

Table 1: Results of XRF analysis, 5 samples of the metamorphic rocks of the region

Sample/Oxides	35	18	28	23	26
SiO_2	50.8	52.5	53	46.7	50.3
Al_2O_3	14.3	13.6	6.3	15.3	11.1
Fe_2O_3	10.3	12.4	10.9	12.8	10.6
MgO	5.9	4.7	13.5	4.7	10.5
CaO	12.3	11.6	12.5	14.6	13.0
SO_3	0.1	0.1	<0.1	0.1	0.2
K_2O	0.3	0.1	<0.1	0.2	0.1
Na_2O	2.9	3.0	0.4	1.3	0.9
TiO2	1.0	0.7	0.4	0.7	0.7
MnO	0.2	0.1	0.2	0.2	0.3
P_2O_5	0.2	0.1	<0.1	0.1	0.1
Cr_2O_3	<0.1	<0.1	0.2	<0.1	0.2
NiO	<0.1	<0.1	0.1	-	<0.1
L.O.I	1.35	0.61	2.04	0.94	1.54
Total	99.85	99.71	99.84	99.44	99.66

Table 2: The results of electron microprobe analysis of garnet in skarn of Dezg

Variables	grt standard	6153-grt1	6153-grt2	6153-grt3	6153-grt5	6153-grt6	6153-grt7	6153-grt8	6153-grt9	6153-grt10
SiO_2	37.85	36.64	37.39	37.10	36.16	36.46	36.35	37.09	37.02	36.27
T_iO_2	0.01	0.60	0.36	0.16	0.57	0.72	0.36	0.79	0.88	1.37
Al_2O_3	21.60	5.22	8.30	8.45	5.38	6.58	4.94	7.16	7.63	6.06
Cr_2O_3	0.00	0.01	0.000	0.00	0.01	0.00	0.00	0.02	0.02	0.01
FeO	32.52	25.17	19.73	19.45	24.89	22.19	24.88	21.43	20.47	23.87
MnO	1.10	0.85	0.20	0.21	0.78	0.48	0.61	0.22	0.18	0.32
MgO	6.02	0.11	0.03	0.03	0.12	0.15	0.07	0.16	0.17	0.15
CaO	0.79	32.47	35.09	34.73	32.39	33.67	33.24	33.44	34.12	33.02
Total	99.89	101.08	101.11	100.14	100.31	100.25	100.45	101.30	100.52	101.01
Formula (Corr.)	12(O)	12(O)	12(O)	12(O)	12(O)	12(O)	12(O)	12(O)	12(O)	12(O)
S_i	2.990	2.932	2.940	2.942	2.913	2.916	2.923	2.927	2.939	2.896
T_i	0.001	0.036	0.021	0.010	0.035	0.043	0.022	0.047	0.052	0.082
Al	2.011	0.492	0.769	0.790	0.511	0.620	0.468	0.666	0.714	0.570
Cr	0.000	0.001	0.00	0.00	0.001	0.00	0.00	0.001	0.001	0.001
Fe+3	0.007	1.571	1.308	1.307	1.591	1.460	1.642	1.385	1.302	1.474
Fe+2	2.141	0.113	-0.011	-0.017	-0.066	-0.024	-0.031	-0.029	-0.057	0.114
Mn	0.074	0.057	0.013	0.014	0.053	0.032	0.041	0.014	0.012	0.022
Mg	0.709	0.013	0.003	0.004	0.014	0.018	0.008	0.018	0.020	0.017
Ca	0.067	2.784	2.956	2.951	2.789	2.886	2.864	2.912	2.902	2.824
XFe_2 (VIII)	0.716	0.038	-0.004	-0.006	0.029	0.008	0.011	0.010	0.019	0.038
XMn (VIII)	0.025	0.019	0.004	0.005	0.018	0.011	0.014	0.005	0.004	0.007
XMg (VIII)	0.237	0.004	0.001	0.001	0.005	0.006	0.003	0.008	0.007	0.006
XCa (VIII)	0.022	0.938	0.948	1.000	0.948	0.975	0.973	0.979	0.0970	0.949
XAl (VI)	0.996	0.239	0.370	0.377	0.243	0.298	0.222	0.325	0.354	0.279
XFe_3 (VI)	0.004	0.761	0.630	0.623	0.757	0.702	0.778	0.675	0.648	0.721
XCr (VI)	0.000	0.000	0.000	0.000	0.000	0.000	0.000	0.000	0.001	0.000
End-members										
Almandine	71.6	3.8	-0.4	-0.8	2.9	0.8	1.1	1.0	1.9	3.800
Spessartine	2.5	1.9	0.4	0.5	1.8	1.1	1.4	0.5	0.4	0.700
Pyrope	23.7	0.4	0.1	0.1	0.5	0.6	0.3	0.8	0.7	0.600
Grossular	2.2	22.4	37.0	37.7	23.0	29.1	21.6	31.8	34.3	26.40
Andradite	0.0	71.4	62.9	62.3	71.8	68.4	57.7	66.1	62.6	68.40
Uvarovite	0.0	0.0	0.0	0.0	0.0	0.0	0.0	0.0	0.1	0.000

transformations of these rocks was carried out based on conversion of minerals into one another and finally by determining different stages of metamorphism and its intensity and extent in the region (Esma'ili, 2014). Five skarn samples were selected for chemical analysis by XRF method. Moreover, microprobe analysis was carried out on 5 rock samples with the maximum degree of metamorphism including minerals garnet, clinopyroxenes, feldspar and amphibole in University of Münster, Germany to determine formation pressure and temperature of skarn (Esmaili, 2014). The results are presented in Table 2 and 3.

Geology and petrography of skarn: In the study region, there are skarns whose main minerals are epidotic, grassular andradite, diopside and calcite and less quartz, sphene and hornblende. These skarns have generally developed inside calc-silicate rock fractures or on the border of limestone, marl, plate and semi-plate rocks.

Formation of such skarns is possible in different metamorphic regions (Kretz, 1994). Formation of these skarns is the result of local metasomatic reactions that happen during regional metamorphism. In this type of skarns like all other skarns; therefore, fluids need to be active in the environment. Intrusive masses are the source of these fluids in common skarns. During prograde metamorphism, decarburization and dehydration reactions occur and amounts of CO_2 and H_2O are produced which move toward the weak points of rocks. These weak points which fluids can flow through and concentrate at are lithologic boundaries (Cartwright, 1994). Cracks in rocks are also a suitable environment are also proper environments for movement and concentration of these fluids. The mentioned fluids mostly dissolve some components of the primary rock and transfer them to the host rock. The fluids derived from limestones are usually full in CO_2 and Ca while fluids obtained from plate rocks may contain some amounts of Fe, K, Na and Si. Entrance of a fluid derived from carbonate rocks to plate rocks or vice versa, results in metasomatism and thus develops skarns and since chemical potential of CO_2 decreases as a result of production of calc-silicate layers and chemical potential of H_2O as a result of production of plate rocks in contact between the two layers of plate rock and calc-silicate (Zhai *et al*., 2014), this areas are suitable environments for reactions that lead to formation of skarns. That is why the above skarns develop in lithologic contact of calc-silicate and carbonate rocks with plate rocks, or in general, in areas containing layers with incompatible composition. On the other hand, a part of

Table 3: The results of electron microprobe analysis of pyroxene in skarns of Dezg

Column 1	6152 px1	6152 px2	6152 px3	6152 px4	6152 px5	6152 px6	6152 px7	6152 px8	6152 px9	6152 px10	6152 px11	6152 px12
SiO_2	55.67	53.24	52.09	52.42	52.74	51.34	52.77	52.44	52.24	52.40	51.30	52.45
T_iO_2	0.00	0.71	0.36	0.25	0.21	0.46	0.21	0.94	0.08	0.01	0.42	0.00
Al_2O_3	10.45	1.548	3.00	2.69	1.11	3.12	2.15	0.68	1.22	1.25	3.40	0.19
Cr_2O_3	0.00	0.00	0.25	0.63	0.07	0.02	0.78	0.02	0.04	0.00	0.35	0.01
FeO	5.05	6.55	6.36	5.08	8.73	7.35	4.52	9.45	10.00	12.43	6.03	12.37
MnO	0.00	0.00	0.19	0.12	0.16	0.12	0.12	0.29	0.32	0.38	0.14	0.44
MgO	8.26	14.06	15.30	16.31	13.56	13.23	16.69	11.97	11.91	10.76	15.81	11.13
CaO	11.18	23.98	22.74	22.31	23.80	24.42	222.98	24.33	24.34	23.62	21.52	24.16
Na_2O	7.70	0.344	0.47	0.21	0.61	0.56	0.18	0.30	0.25	0.35	0.19	0.22
K_2O	0.00	0.00	0.08	0.00	0.00	0.00	0.02	0.01	0.04	0.01	0.00	0.00
Total	96.33	100.094	100.83	100.01	100.99	100.62	100.41	100.43	100.45	101.22	99.56	101.42
Fomula	6(O)	6(O)	6(O)	6(O)	6(O)	6(O)	6(O)	6(O)	6(O)	6(O)	6(O)	6(O)
Si	2.051	1.970	1.912	1.924	1.958	1.906	1.929	1.968	1.955	1.972	1.899	1.977
Ti	0.000	0.002	0.010	0.007	0.006	0.013	0.006	0.027	0.002	0.000	0.012	0.000
Al	0.454	0.072	0.130	0.116	0.049	0.137	0.093	0.030	0.054	0.056	0.0148	0.008
Cr	0.000	0.000	0.007	0.018	0.002	0.001	0.022	0.001	0.001	0.000	0.010	0.000
Fe3+	0.000	0.000	0.000	0.000	0.000	0.000	0.000	0.000	0.000	0.000	0.000	0.000
Fe2+	0.154	0.203	0.195	0.156	0.271	0.228	0.138	0.297	0.314	0.391	0.187	0.390
Mn	0.000	0.006	0.006	0.004	0.005	0.004	0.003	0.009	0.010	0.012	0.004	0.014
Mg	0.344	0.776	0.837	0.892	0.751	0.732	0.909	0.570	0.668	0.604	0.873	0.626
Ca	0.442	0.951	0.894	0.877	0.947	0.972	0.900	0.978	0.981	0.952	0.870	0.994
Na	0.550	0.025	0.033	0.015	0.044	0.040	0.013	0.022	0.019	0.026	0.014	0.016
K	0.000	0.000	0.004	0.000	0.000	0.000	0.001	0.000	0.002	0.000	0.000	0.000
Total	3.997	4.004	4.028	4.009	4.033	4.032	4.015	4.001	0.016	4.013	4.017	4.026
Tri plots												
En	0.365	0.402	0.435	0.463	0.381	0.379	0.467	0.344	0.340	0.310	0.452	0.311
Fs	0.165	0.105	0.101	0.081	0.138	0.118	0.071	0.153	0.160	0.201	0.097	0.194
Wo	0.469	0.493	0.464	0.458	0.481	0.503	0.462	0.503	0.500	0.489	0.451	0.495
Jd	0.550	0.025	0.031	0.013	0.043	0.040	0.010	0.021	0.019	0.026	0.013	0.015
Ac	0.000	0.000	0.002	0.002	0.002	0.000	0.003	0.000	0.000	0.000	0.001	0.001
Aug	0.450	0.975	0.957	0.985	0.965	0.960	0.987	0.978	0.981	0.974	0.986	0.984
A (+aqw)	0.054	0.012	0.026	0.030	0.002	0.024	0.026	0.002	0.009	0.008	0.036	0.002
C (+aqw)	0.494	0.485	0.451	0.441	0.479	0.490	0.450	0.500	0.493	0.482	0.434	0.492
(FM) (+aqw)	0.559	0.503	0.523	0.529	0.519	0.586	0.525	0.498	0.498	0.510	0.530	0.510
Mole fractions												
XSi (T)	1.000	1.000	1.000	1.000	1.000	1.000	1.000	1.000	1.000	1.000	1.000	1.000
XAl (T)	0.000	0.000	0.000	0.000	0.000	0.000	0.000	0.000	0.000	0.000	0.000	0.000
XAl (M1)	0.454	0.072	0.130	0.116	0.049	0.137	0.093	0.030	0.054	0.056	0.148	0.000
XFe_3 (M1)	0.000	0.000	0.000	0.000	0.000	0.000	0.000	0.000	0.000	0.000	0.000	0.008
XFe_2 (M1)	0.154	0.197	0.177	0.139	0.260	0.223	0.125	0.296	0.310	0.378	0.163	0.384
XMg (M1)	0.340	0.753	0.759	0.793	0.720	0.717	0.822	0.669	0.658	0.683	0.763	0.616
XFe_2 (M2)	0.002	0.006	0.018	0.017	0.011	0.005	0.013	0.000	0.005	0.013	0.023	0.006
XMg (M2)	0.004	0.023	0.078	0.100	0.030	0.016	0.087	0.000	0.010	0.021	0.109	0.010
XCa (M2)	0.442	0.951	0.894	0.877	0.947	0.972	0.900	0.978	0.981	0.952	0.870	0.994
XNa (M2)	0.550	0.025	0.033	0.015	0.044	0.040	0.013	0.022	0.019	0.026	0.014	0.016

fluids also travel into cracks and fractures of surrounding rocks, react with host rocks and form skarns that are limited to fractures. In the Workshop of Skarn Deposits, a model for formation of skarns was proposed which is presented in Fig. 2 which is in fact a summary of the above discussion on how skarns form.

In Dezg region, skarn has developed inside intrusive masses or calc-silicate rock fractures. According to the abovementioned information and the model proposed in Workshop of Skarn Deposits presented in Fig. 2, formation of skarns in the region can be attributed to the function of the intrusive masses and contact metamorphism.

In these skarns, large hypidiomorphic pink crystals of garnet can be observed such that abundance of garnet gives a bright muddy color to the rock. These skarns are well developed in southeast and east areas of Dezg. Microscopic examinations indicated that the major part of the rock is composed of garnet minerals (Fig. 3), clinopyroxene and plagioclase formed in parts with epidote section are also observed which may be as a result of retrograde metamorphism. Garnets belong to ugrandite (andradite grossular) group and form the main part of shaped and amorphous rocks. Quartz and clay minerals are also present; however, their amount is limited. Almost all of these rocks are affected by the solutions derived from intrusive igneous masses which led to contact metamorphism and formation of skarn.

Two types of alteration in skarn system include primary prograde stage which is associated with anhydrous minerals like garnet and pyroxene and final retrograde stage which is characterized by hydrous

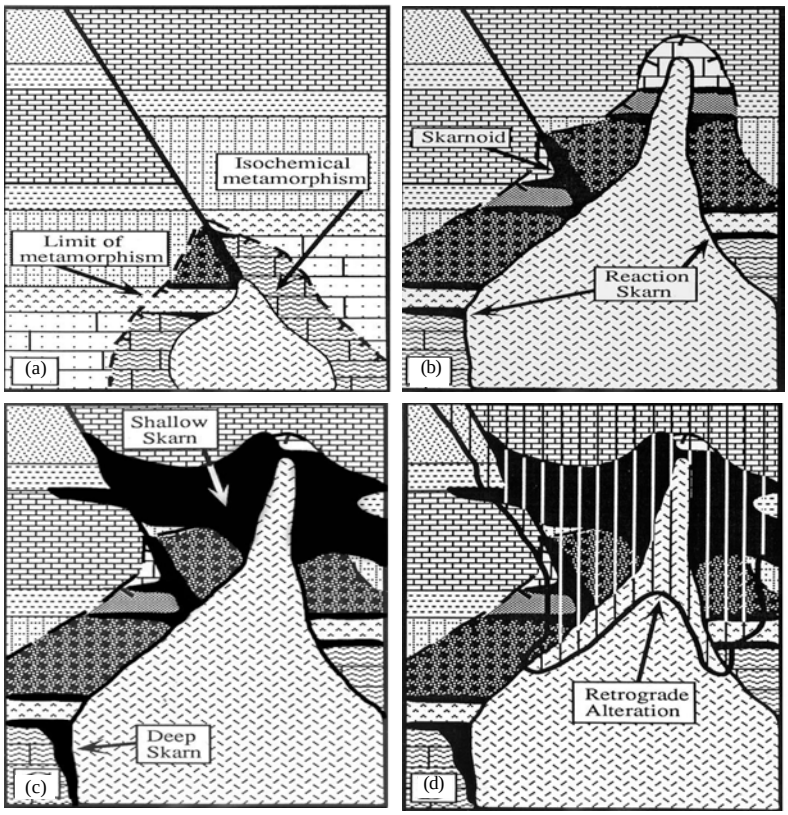

Fig. 2: a-d) The model of skarn formation in the study region

minerals including epidote, hornblende, calcite, quartz and chlorite. In prograde stage, due to deposit of anhydrous calcium silicate minerals andradite, grossular and clinopyroxene, the temperature range between 756 and 776°C and XCO_2 = 0.1-0.6 can be expressed. In retrograde metamorphism at temperatures lower than 756°C, an assemblage of anhydrous calcium silicate minerals turn into hydrous silicate minerals like epidote minerals. And finally, the assemblage of hydrous and anhydrous calcium silicate minerals undergo metamorphism and turn into fine mineral assemblages like chlorite, calcite and quartz and clay minerals.

Mineral chemistry of metamorphic rocks: In this stduy mineral chemistry of metamorphic rocks of the region studied using electron microprobe analysis in University of Münster, Germany is presented. The results of electron microprobe analysis of these minerals are presented in Table 2 and 3.

Garnet: Garnet is one of the main skarn minerals in Dezg. Table 2 presents the results of electron microprobe analysis of garnet in skarn sample of Dezg. Based on the

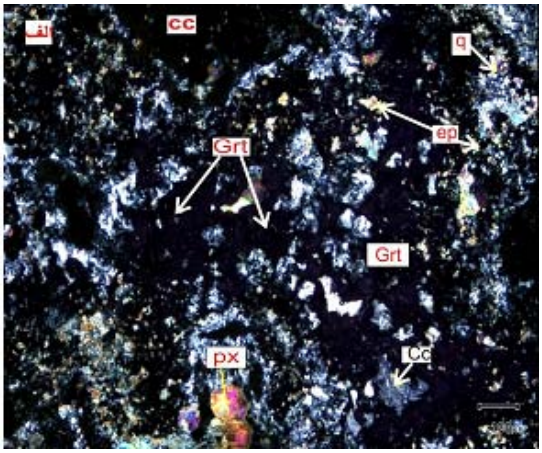

Fig. 3: Skarn garnets in southwest of Dezg

collected field data, it was concluded that rock units in this region are affected by tectonic activities. Therefore, under the influence of shearing activity of minor faults, cracks and fractures form in limestones. This permeable network is an important factor for leakage of hydrothermal solutions and mineralization of calcium garnets by providing channels for flow of magmatic volatiles or

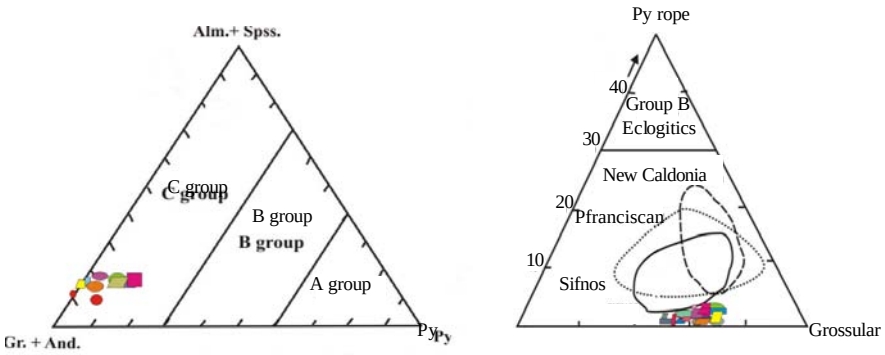

Fig. 4: Index diagram of skarn garnets in southwest of Dezg (Derived from

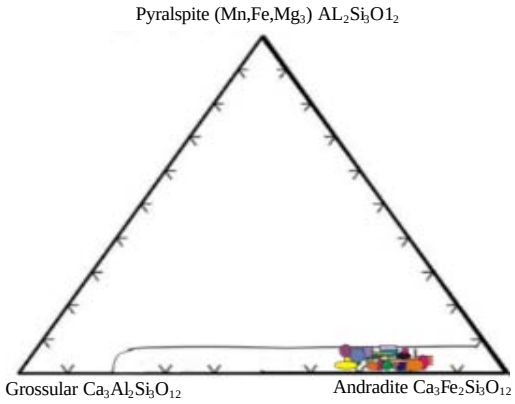

Fig. 5: The position of the garnets in andradite grossular area

volatiles and products obtained from thermal metamorphic reactions. Figure 4 and 5 percent composition of garnets in relevant diagrams. Garnet is from index minerals of skarns in Dezg. Since this mineral forms in the final stages of mineralization, it is almost seen in different Subhedral to Euhedral shapes.

Pyroxene: The results of electronic micro-processing analysis of clinopyroxenes of the study region are presented in Table 3. According to Fig. 6, composition of clinopyroxenes is the same and places in the field of diopside to augite diopside and hedenbergite. According to the diagram presented in Fig. 7, all clinopyroxenes have metamorphic nature which indicates that this mineral is crystalized in metamorphism conditions. The rate of changes in Al_2O_3 was from 0.16 to 5.61 weight percent (Wt%) and Ca_O changes from 21.4-25.06 Wt%.

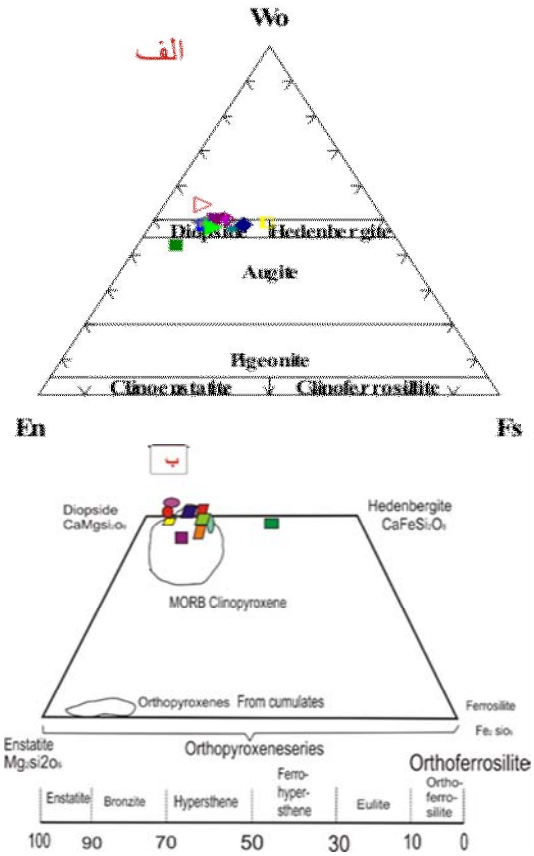

Fig. 6: a) Variations of clinopyroxene composition in skarn samples existing in southeast of Dezg; b) Quadrilateral chart of pyroxenes which indicate the presence of diopside and augite diopside in skarn samples

Geothermobarometry: One of the issues that has nowadays developed in metamorphic rocks is to determine the formation pressure and temperature of rocks (thermobarometry). A method to estimate the formation pressure temperature of minerals in balance state is to use individual thermobarometer which is independently

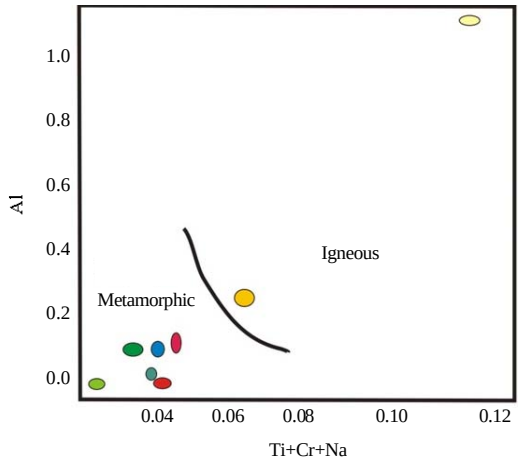

Fig. 7: Cr+Na+Ti compared to Al indicates that more clinopyroxenes have metamorphic nature

regulated based on experimental or thermodynamic data. In order to measure the formation temperature and pressure of mineral assemblages in the present study, thermobarometers with balanced pair minerals or single minerals were employed (Krogh, 1988). Figure 1 is the simplified geology of the study region and indicates exposure of rock samples on which thermobarometry have carried out.

Geothermobarometry based on a type of pyroxene: Mercier (1980) proposed thermometers and barometers based on clinopyroxene or orthopyroxene to be used to determine crystallization temperature and pressure of garnet peridotites and spinel peridotites. These calibrations are based on the effect of Cr on solubility of Al. Therefore, these thermometers and barometers are applicable for chromium-rich mineral assemblages (Sutthirat, 2001). These single-pyroxene thermometers and barometers are designed based on thermodynamic principles. Following equations are true for clinopyroxenes:

$$T_{CPX}(°C) = \left[(-7537.5\,A\log X_{KW} + 61152)/D\right] - 273$$

$$P_{CPX}(Kb) = \left[\left(\begin{array}{c} 419.76\,A\log X_{KW} - 706.14 \\ A\log X_{KA} + 616.61 \end{array}\right)\right]/D$$

That:

$$X_{KW} = (1-2W)/(0.667 + 0.667W)$$

$$X_{KA} = A/(1-A)(1-1.27\,F_{Cr})$$

$$D = A\log X_{KA} A\log X_{KW} - 11.2724\,A\log X_{KW} + 2.2595\,A\log X_{KA} + 2.371$$

$$W = Ca/(Ca(+Mg + Fe^{2+} + Mn),$$

$$A = (Al - Na)/2,\ F_{Cr} = Cr/(Al + Cr - Na)$$

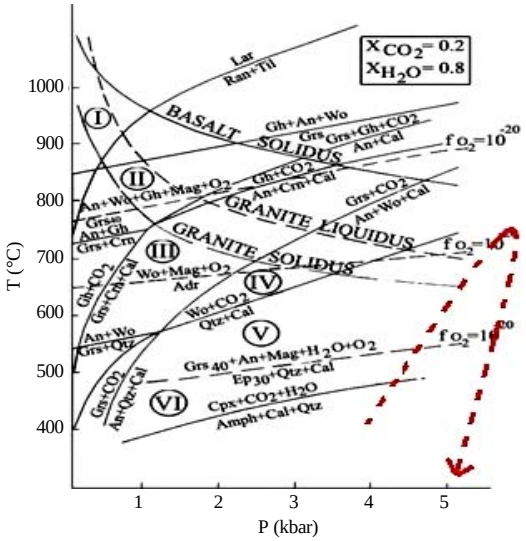

Fig. 8: The range of the facies in the skarn, in diagram P-T [33]

Geothermobarometry and discussion: In the studied metamorphic rocks, according to the balanced minerals in different metamorphic facies and by using the results of microprobe analyses, the activity of end organs of mineral can be achieved through "Active.exe" software for end organs of each mineral, then, Ptmafic software is employed to determine formation and crystallization temperature and pressure of mineral assemblages of these rocks (Soto and Soto, 1995).

The results of geothermobarometry in skarn samples: Based on the microprobe data and the relevant software, the obtained temperatures and pressures are presented in Table 4-6. The range of the conducted reactions and the taken path are indicated in Fig. 8. Therefore, 5 (pyroxene-garnet facie) and VI (pyroxene epidote facie) can be observed in the study region. The consequences of retrograde metamorphism under the influence of hydrothermal, metamorphic or cooler climate fluids full in H_2O result in formation of hydrous minerals like epidote. Conversion of garnet into epidote and pyroxene into actinolite and chlorite can be evidence for occurrence of retrograde metamorphism in evolution of skarn in the region. According to the diagram presented in Fig. 8, metamorphism of skarn in the region is of average degree. Figure 8 which is the range of the facies in skarn in diagram P-T, the boundary between the facies is indicated using a series of key reactions. In general, two facies of hornblende hornfels and albite epidote-hornfels can be observed.

Hornblende-hornfels facie: This facie formed in a temperature between 420 and 925°C and pressure of 3-5 Kb. Yardley (1981) believes that hornblende-hornfels

Table 4: The results obtained from calculation of temperature in the software on pyroxenes available in skarns (Newton and Parkins III, 1982; Holland and Powell, 1985; Raheim and Green, 1974)

Variables	S1	S2	S3	S4	S5	S6	S7	S8	S9	S10	S11
Raheim and Green (1974)	477.80	435.8	643.33	2175.83	1011.23	1054.27	1172.8	1241.98	118.83	763.81	906.568
Holland and Powell (1985)											
Kerogh (1988)	327.93	308.98	494.11	3178.99	906.32	953.07	1105.89	1209.6	123.55	599.36	921.68
Newton and Parkins III (1982)											
Sengupta *et al.* (1989)	221.08	208.98	315.44	885.06	487.95	502.93	545.76	578.83	87.24	362.37	419.564
Raheim and Green (1974)											
rFe	3.3040	3.535	3.923	4.500	9.107	4.187	4.35	4.258	0.775	4.306	4.2245
rMg	1.7100	1.057	1.025	1.007	1.018	1.016	1.013	1.014	3.041	1.014	1.2276

Table 5: The results obtained from calculation of pressure in the software by garnet-pyroxene-plagioclase method in skarn (Soto and Soto, 1995; Sutthirat, 2001; Tirrul *et al.*, 1983; Yardley, 1981)

Garnet-pyroxene- plagioclase	C/S1	C/S2	C/S3	C/S4	C/S5	C/S6	C/S7	C/S8	C/S9	C10/Average
Perkins III and Newton (1981), Soto and Soto (1995), Newton and Perkins III (1982) and Sutthirat (2001)	6.4	1.54	2.75	3.71	22	2.58	8.61	3.42	6.4	3.90125
Holland and Powell (1985) and Tirrul *et al.* (1983)	8.71	1.9	3.19	4.21	2.55	2.98	9.39	12.199	0.1	4.564875
Eckert (1991) and Yardley (1981)	9.22	3.52	4.79	6	4.5	4.67	11.57	5.69	1.91	5.33125

Table 6: The results obtained from calculation of temperature in the software by garnet-amphibole method (Zhai *et al.*, 2014)

Garnet-amphibole	T(°C)
Graham and Powell (1984) and Zhai *et al.* (2014)	883.72
Perchuck *et al.* (1985)	385.37

facie can be named low pressure amphibolite facie. Mineral paragenesis diopside+calcite places in the end of this facie and in the beginning of pyroxene-hornfels facie. In the study region, the mineral assemblage of calcite+clinopyroxene+garnet+ferro-actinolite can be attributed to this facie.

Albite epidote-hornfels facie: This facie belongs to the lowest temperature of contact metamorphic facies. Index minerals of this facie in the region include calcite, quartz, garnet, ferro-actinolite and chlorite.

RESULTS AND DISCUSSION

The results of the present study are as follow. According to the data of microprobe analysis, the garnets available in the skarn are andradite-grossular and have been formed at the expense of clinopyroxene. The composition skarn clinopyroxenes is diopside to augite diopside and hedenbergite. According to the results of the analyses, all clinopyroxenes have metamorphic nature which indicates that this mineral is crystalized in metamorphic conditions. According to the results of thermobarometry studies, rock units of the region are of average pressure and temperature type. Two types of alteration in skarn system include primary prograde stage which is associated with anhydrous minerals like garnet and pyroxene and final retrograde stage which is characterized by hydrous minerals including epidote, hornblende, calcite, quartz and chlorite. Formation of anhydrous calcium silicate minerals like andradite, grossular and clinopyroxene proves the temperature range between 756 and 776°C and XCO_2 = 0.1-0.6. In retrograde metamorphism at temperatures lower than 756°C, an assemblage of anhydrous calcium silicate minerals turn into hydrous silicate minerals like epidote minerals. And finally, the assemblage of hydrous and anhydrous calcium silicate minerals undergo metamorphism and turn into fine mineral assemblages like chlorite, calcite and quartz and clay minerals. Based on the minerals and temperature-pressure calculations of the skarn under investigation, two facies of hornblende-hornfels and albite epidote-hornfels were identified in this rock assemblage.

CONCLUSION

The presence of intergrowth texture and absence of replacement texture in andradite and pyroxene is showing that these minerals are formed as contemporaneous. This mineral assmbelage has crystallized in high partial water pressure which is between 0.8-0.9 whole pressure. High partial water pressure has been certainly result of water fluid seepage from granitic body to country rock.

ACKNOWLEDGEMENT

Sincere thanks go to Prof. Michael Brooker and Mr. Timan who helped with electron microprobe analysis of the samples in University of Münster, Germany.

REFERENCES

Angiboust, S., P. Agard, J.C.M. De Hoog and J. Omrani and A. Plunder, 2013. Insights on deep, accretionary subduction processes from the Sistan ophiolitic melange (Eastern Iran). Lithos, 156: 139-158.

Brocker, M., G.F. Rad, R. Burgess, S. Theunissen and I. Paderin *et al.*, 2013. New age constraints for the geodynamic evolution of the Sistan Suture Zone, Eastern Iran. Lithos, 170: 17-34.

Cartwright, J.A., 1994. Episodic basin-wide hydrofracturing of overpressured Early Cenozoic mudrock sequences in the North Sea Basin. Mar. Pet. Geol., 11: 587-607.

Eckert, J.O.J.R., R.C. Newton and O.J. Kleppa, 1991. Heat of reaction and recalibration of garnet-pyroxene-plagioclase-quartz geobarometers in CMAS system by solution calorimetry of stoichiometric mineral mixes. Am. Mineral., 79: 148-160.

Esmaili, Z., 2014. Petrology of metamorphic rocks in Dezg (southwest of Shahrokht) East of Iran. MSc Thesis, University of Birjand, Birjand, Iran.

Graham, C.M. and R. Powell, 1984. A garnet-hornblende geothermometer: Calibration, testing and application to the Pelona Schist, Southern California. J. Metamorph. Geol., 2: 13-31.

Holland, T.J.B. and R. Powell, 1985. An internally consistent thermodynamic dataset with uncertainties and correlations: 2 Data and results. J. Metamorph. Geol., 3: 343-370.

Kretz, R., 1994. Metamorphic Crystallization. John Wiley & Sons, Chichester, England,.

Krogh, E.J., 1988. The garnet-clinopyroxene Fe-Mg geothermometer a reinterpretation of existing experimental data. Contrib. Mineral. Petrol., 99: 44-48.

Mercier, J.C.C., 1980. Single-pyroxene thermometry. Tectonophysics, 70: 1-37.

Newton, R.C. and D. Perkins III, 1982. Thermodynamic calibration of geobarometers based on the assemblages garnet-plagioclase-orthopyroxene (clinopyroxene)-quartz. Am. Mineral., 67: 203-222.

Perchuck, L.L., L.Y. Aranovich, K.K. Podlesskii, I.V. Lavaranteva and V.Y. Gerasimov *et al*., 1985. Precambrian granulites of the Aldan Shield, Eastern Siberia, USSR. J. Metamorph. Geol., 3: 265-310.

Perkins, D. III. and R.C. Newton, 1981. Charnockite geobarometers based on coexisting garnet pyroxene plagioclase quartz. Nat., 292: 144-146.

Rad, G.F., G.T.R. Droop, S. Amini and M. Moazzen, 2005. Eclogites and blueschists of the Sistan Suture Zone, Eastern Iran: A comparison of P-T histories from a subduction melange. Lithos, 84: 1-24.

Rad, G.R., G.T.R. Droop and R. Burgess, 2009. Early cretaceous exhumation of high-pressure metamorphic rocks of the Sistan Suture Zone, Eastern Iran. Geol. J., 44: 104-116.

Raheim, A. and D.H. Green, 1974. Experimental petrology of lunar highland basalt composition and applications to models for the lunar interior. J. Geol., 82: 607-622.

Sengupta, P., S. Dasgupta, P.K. Bhattacharya and Y. Hariya, 1989. Mixing behavior in quaternary garnet solid solution and an extended Ellis and Green garnet-clinopyroxene geothermometer. Contrib. Mineral. Petrol., 103: 223-227.

Soto, J.I. and V.M. Soto, 1995. PTMAFIC: Software package for thermometry, barometry and activity calculations in mafic rocks using an IBM-compatible computer. Comput. Geosci., 21: 619-652.

Sutthirat, C., 2001. Petrogenesis of mantle and crustal xenoliths and xenocrysts in basaltic rocks associated with corundum deposits in Thailand. Ph.D Thesis, University of Manchester, Manchester, England.

Tirrul, R., I.R. Bell, R.J. Griffis and V.E. Camp, 1983. The sistan suture zone of Eastern Iran. Geol. Soc. Am. Bull., 94: 134-156.

Yardley, B.W., 1981. Effect of cooling on the water content and mechanical behavior of metamorphosed rocks. Geol., 9: 405-408.

Zhai, D., J. Liu, J. Wang, Y. Yang and H. Zhang *et al*., 2014. Zircon U-Pb and molybdenite Re-Os geochronology and whole-rock geochemistry of the Hashitu molybdenum deposit and host granitoids, Inner Mongolia, NE China. J. Asian Earth Sci., 79: 144-160.